LECTURE 29

Phosphorus Loading Concept

FIGURE 29.1
Vollenweider's (1968) loading plot.
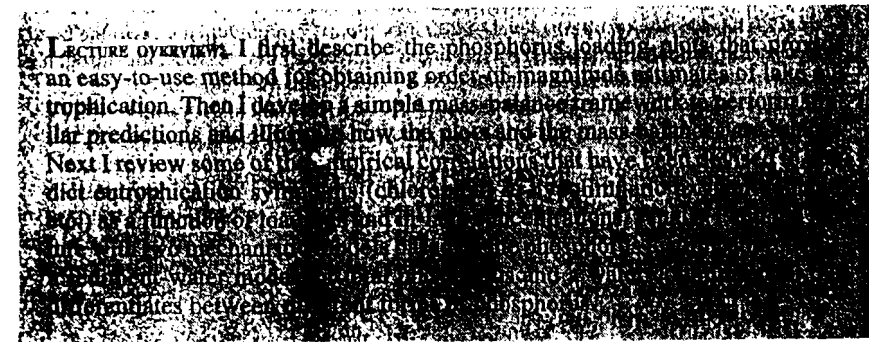
The phosphorus loading concept is based on the premise that phosphorus is the primary, controllable limiting nutrient of lake and reservoir eutrophication. A number of simple empirical models have been developed to predict lake eutrophication on the basis of this premise. The earliest and most fundamental were developed by Richard Vollenweider. As a consequence they are often termed "Vollenweider plots."

29.1   VOLLENWEIDER LOADING PLOTS

The first loading plot was developed by Vollenweider (1968). This model was based on Rawson's (1955) insight that deeper lakes are less susceptible to eutrophication than shallower systems. Vollenweider compiled areal loadings of total phosphorus L_p (mgP m^{-2} yr^{-1}) and mean depth H (m) from north temperate lakes from around the world. He used these points to locate the lakes on a space defined by log L_p versus log H (Fig. 29.1). He then labeled each lake as to its trophic status (oligotrophic, mesotrophic, eutrophic). Finally he superimposed lines dividing the various categories of lakes.
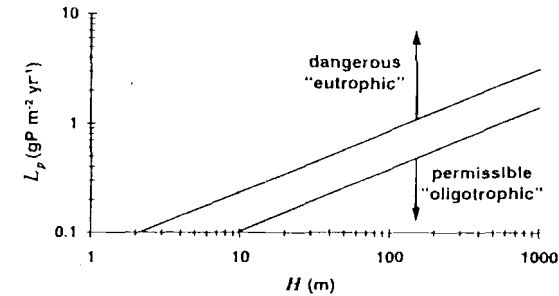
As displayed in Fig. 29.1, the plot provides an easy-to-use model to perform both simulation and wasteload allocation calculations for lakes. For a simulation calculation the modeler would use loading and depth data to predict trophic state. For a wasteload allocation calculation the modeler would determine the loading required to attain a desired trophic state for a lake of a particular mean depth.

In a subsequent paper Vollenweider (1975) added a second determining factor into the loading plot framework. He recognized that not only depth but also residence time had an impact on eutrophication. In essence he observed that faster flushing lakes seemed to be less susceptible to eutrophication than lakes with long residence times. He incorporated this effect into the plot by adding the inverse residence time to the abscissa.

As in Fig. 29.2, he again plotted lakes on this space and superimposed lines. However, along with straight lines, he suggested that curves represented a superior fit of the data. Again, as with the earlier version (Fig. 29.1), the plot can be used for both simulation and wasteload allocation predictions.

It should be noted that one problem with using mean depth and residence time is that they are not independent. In fact, the abscissa, H/τ_w, can be shown to be independent of depth,

$$\frac{H}{\tau_w} = \frac{HQ}{V} = \frac{HQ}{HA_s} = \frac{Q}{A_s} \equiv q_s \tag{29.1}$$

where q_s is called the hydraulic overflow rate (m yr^{-1}). Note that engineers involved in water and waste treatment have historically correlated sedimentation in treatment reactors with the overflow rate (Reynolds 1982).

A final refinement was developed independently by Vollenweider (1976) and Larsen and Mercier (1976). Their models corresponded to plots of the logarithm of L_p versus the logarithm of $q_s(1 + \sqrt{\tau_w})$. Again, curves were used to divide the loading levels on the plot.

Other investigators, notably Rast and Lee (1978), have applied Vollenweider's (1976) approach to larger data bases and have extended it to predict trophic status. We review these extensions in Sec. 29.3.
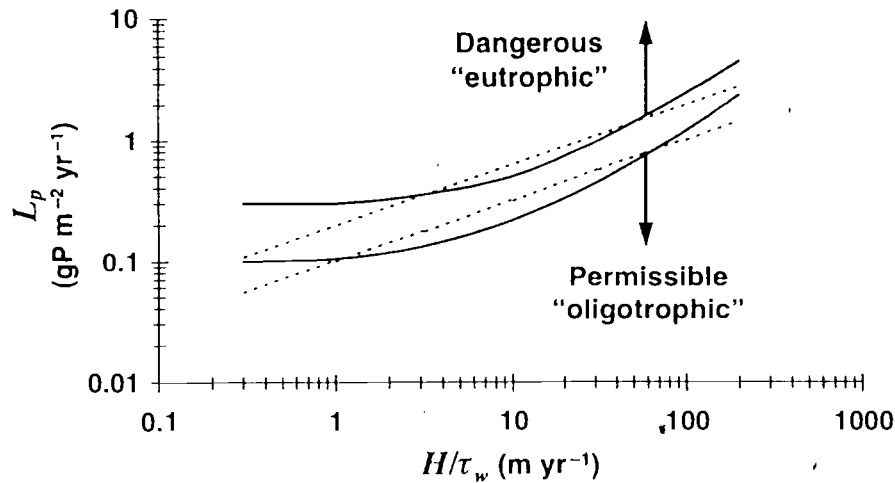
FIGURE 29.2
Vollenweider's (1975) loading plot.

29.2 BUDGET MODELS

Early in the development of phosphorus loading models, it was recognized that simple mass-balance models could provide the same predictions as loading plots. In fact Vollenweider (1976) wrote one of the first phosphorus mass-balance models for a well-mixed lake as

$$V\frac{dp}{dt} = W - Qp - k_s Vp \qquad (29.2)$$

where V = volume (m³)
  p = total phosphorus concentration (mg m⁻³)
  t = time (yr)
  W = total P loading rate (mg yr⁻¹)
  Q = outflow (m³ yr⁻¹)
  k_s = a first-order settling loss rate (yr⁻¹)

At steady-state this equation can be solved for

$$p = \frac{W}{Q + k_s V} \qquad (29.3)$$

Based on phosphorus budget data (that is, inputs, outputs, and concentration of phosphorus), the loss rate can be determined as

$$k_s = \frac{W - Qp}{Vp} = \frac{W}{Vp} - \frac{1}{\tau_w} \qquad (29.4)$$

On the basis of such budget calculations, Vollenweider concluded that the loss rate could be approximated by

$$k_s = \frac{10}{H} \qquad (29.5)$$

Chapra (1975) suggested that because the loss of phosphorus was due to settling of particulate phosphorus, the loss term should be represented as

$$V\frac{dp}{dt} = W - Qp - vA_s p \qquad (29.6)$$

where v is the apparent settling velocity (m yr⁻¹). If this is true, at steady-state Eq. 29.6 can be solved for

$$p = \frac{W}{Q + vA_s} \qquad (29.7)$$

Thus we can see that Vollenweider's estimate that $k_s = 10/H$ supports the settling velocity approach. In fact Eq. 29.5 is equivalent to using Eqs. 29.6 and 29.7 with $v = 10$ m yr⁻¹. Data analysis by a number of individuals (e.g., Chapra 1975, Dillon and Rigler 1975, Thomann and Mueller 1987) has determined that the settling velocity most commonly takes on values in the range from about 5 to 20 m yr⁻¹. However, values have been reported from less than 1 to over 200 m yr⁻¹.

The unity between loading plots and budget models can be illustrated (Chapra and Tarapchak 1976) by dividing the numerator and denominator of Eq. 29.7 by the surface area to give

$$p = \frac{L}{q_s + v} \qquad (29.8)$$

or

$$L = p(q_s + v) \qquad (29.9)$$

Taking the logarithm of Eq. 29.9 gives

$$\log L = \log p + \log(q_s + v) \qquad (29.10)$$

It is assumed that for phosphorus-limited systems, trophic state is correlated with phosphorus concentrations. Vollenweider and others have suggested that mesotrophy is bounded by total phosphorus concentrations of 10 and 20 μgP L⁻¹ (Table 29.1). If this is true, Eq. 29.10 can be used to draw lines on a graph of $\log L_p$ versus $\log q_s$. As in Fig. 29.3, the result is a loading plot that is quite similar to Vollenweider's (1975) model.

Beyond showing the unity of the two approaches, the budget approach is useful in elucidating the mechanisms that underlie the shape of the loading plot. Inspecting Eq. 29.10 indicates that there are two asymptotes. At one extreme (low flushing lakes; small q_s) Eq. 29.10 reduces to

$$\log L = \log p + \log v = \text{constant} \qquad (29.11)$$

Thus as assimilation becomes solely dependent on sedimentation, the curves flatten out on the left side of Fig. 29.3. Conversely for high flushing lakes (high q_s), Eq. 29.10 approaches

TABLE 29.1

Trophic-state classification based on total phosphorus concentration as well as on other variables reflective of eutrophication

Variable	Oligotrophic	Mesotrophic	Eutrophic
Total phosphorus (μgP L^{-1})	< 10	10–20	> 20
Chlorophyll a (μgChla L^{-1})	< 4	4–10	> 10
Secchi-disk depth (m)	> 4	2–4	< 2
Hypolimnion oxygen (% saturation)	> 80	10–80	< 10

$$\log L = \log p + \log q_s \qquad (29.12)$$

Consequently, as assimilation becomes solely dependent on flushing, the curves approach straight lines with a slope of one.

Beyond the Vollenweider (1975) plot, the above theoretical development can be employed to gain insight into his 1976 model, which can be formulated as
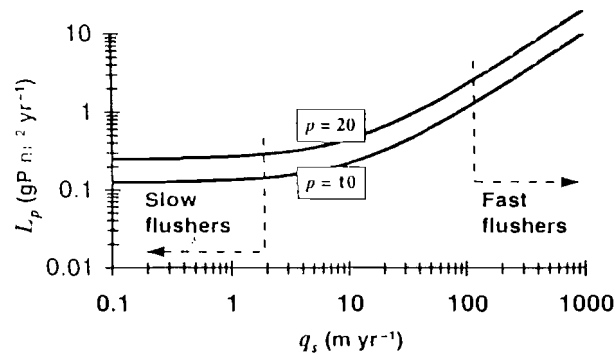
$$p = \frac{L \cdots}{q_s(1 + \sqrt{\tau_w})} \qquad (29.13)$$

Comparing Eqs. 29.8 and 29.13 leads to the conclusion that the 1976 model has a settling velocity

$$v = q_s \sqrt{\tau_w} = \frac{H}{\sqrt{\tau_w}} \qquad (29.14)$$

or a first-order rate of

$$k_s = \frac{1}{\sqrt{\tau_w}} \qquad (29.15)$$

FIGURE 29.3
Loading plot derived from a phosphorus budget model (Eq. 29.10 with $v = 12.4$ m yr^{-1}).

29.3 TROPHIC-STATE CORRELATIONS

In the previous sections we calculated total phosphorus concentrations and interpreted the resulting levels as indicators of trophic status. Another approach is to use phosphorus concentration (or in some cases loadings) to predict other trophic-state variables that more directly reflect the deleterious effects of eutrophication.

As in Table 29.1, these other variables provide measures of eutrophication. In fact because they are more directly reflective of the adverse effects of eutrophication, they are preferable to total phosphorus concentration.
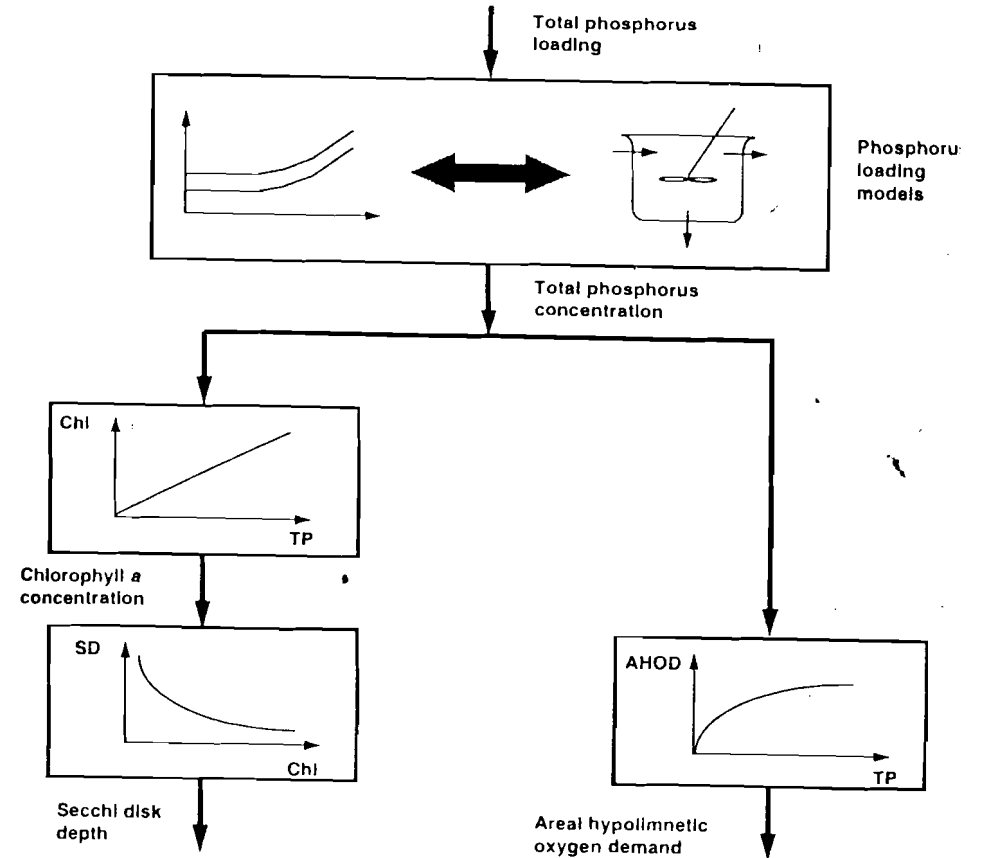
FIGURE 29.4
Schematic of approach used by Chapra (1980) to predict trophic state variables based on phosphorus loading model predictions. The approach consists of a number of submodels and correlations that form a hypothesized causal chain that starts with total P concentration predictions based on budget models or loading plots. This concentration is used in conjunction with a series of correlation plots to estimate symptoms of eutrophication such as chlorophyll a concentration, Secchi-disk depth, and hypolimnetic oxygen demand.

One such scheme is outlined in Fig. 29.4. The approach consists of relating predicted total phosphorus concentrations to symptoms of eutrophication such as chlorophyll a concentration, Secchi-disk depth, and hypolimnetic oxygen demand. Each step is dictated by empirically derived correlations, as described next.

29.3.1 Phosphorus-Chlorophyll Correlations

Initial attempts to extend phosphorus loading models attempted to calculate chlorophyll a levels as a function of total P concentration. Most of these are based on a fit of a log-log plot. Several examples are

Dillon and Rigler (1974):

$$\log(\text{Chl}a) = 1.449 \log(p_v) - 1.136 \tag{29.16}$$

Rast and Lee (1978):

$$\log(\text{Chl}a) = 0.76 \log(p) - 0.259 \tag{29.17}$$

Bartsch and Gakstatter (1978):

$$\log(\text{Chl}a) = 0.807 \log(p) - 0.194 \tag{29.18}$$

where Chl$a$ = chlorophyll a concentration (μg L^{-1})
  p = total P concentration (μg L^{-1})
  p_v = spring total P concentration (μg L^{-1})

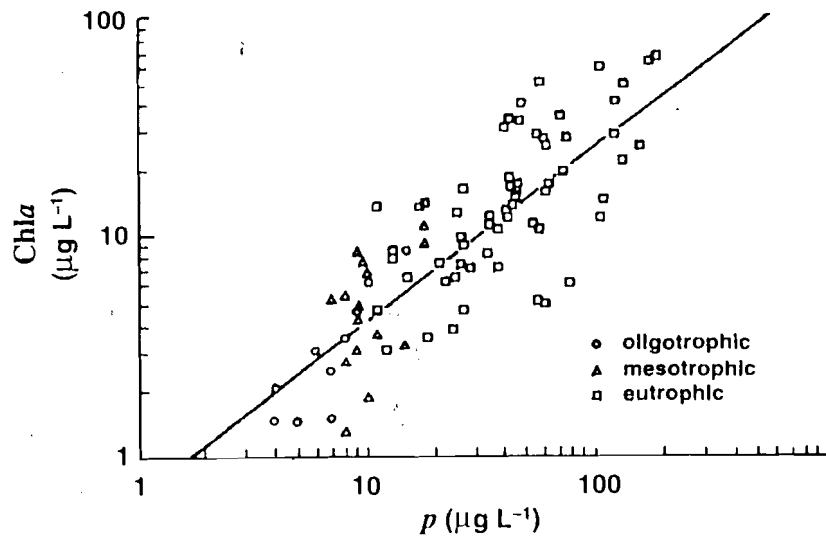Figure 29.5 shows the Bartsch and Gakstatter (1978) version.

FIGURE 29.5
The relationship between chlorophyll a and phosphorus in some United States lakes and reservoirs (from Bartsch and Gakstatter 1978).

All these models show an increase of chlorophyll with increasing phosphorus. In all cases the relationship is nonlinear. However, the Dillon and Rigler model differs in that its exponent is greater than 1 (slope of log-log plot = 1.449), connoting that more polluted lakes exhibit proportionately higher chlorophyll than less polluted lakes. The other correlations show less chlorophyll per phosphorus for more productive systems.

In addition all the models are assumed to be appropriate only for phosphorus-limited systems. Smith and Shapiro (1981) have presented a modified correlation that attempts to account for potential nitrogen limitation,

$$\log(\text{Chl}a) = 1.55 \log(p) - b \tag{29.19}$$

where

$$b = 1.55 \log\left[\frac{6.404}{0.0204(\text{TN:TP}) + 0.334}\right] \tag{29.20}$$

in which TN:TP = total nitrogen to phosphorus ratio.

29.3.2 Chlorophyll-Secchi-Disk Depth Correlations

Attempts to relate Secchi-disk depth to chlorophyll levels have again usually started with log-log plots. One such graph is shown in Fig. 29.6, and it can be described by the equation

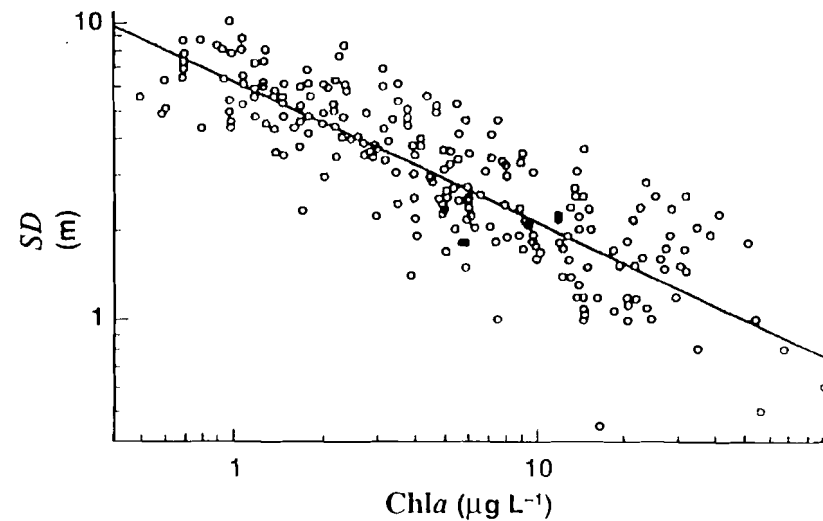$$\log(SD) = -0.473 \log(\text{Chl}a) + 0.803 \tag{29.21}$$

FIGURE 29.6
The relationship between Secchi-disk depth and chlorophyll a (from Rast and Lee 1978).

where SD = Secchi-disk depth (m).

When this equation is transformed into normal coordinates, it becomes

$$SD = 6.35 \text{Chl} a^{-0.473} \qquad (29.22)$$

Thus the fit traces out a hyperbolic shape that, as expected, exhibits large Secchi-disk depths at low chlorophyll concentrations and small Secchi-disk depths at high chlorophyll concentrations.

The shape can be related to more fundamental measurements by recognizing that light extinction in natural waters is often described by the Beer-Lambert law

$$I = I_0 e^{-k_e H} \qquad (29.23)$$

where I = light at depth H

I_0 = light at the surface

k_e = extinction coefficient of the water

A number of investigators have related Secchi-disk depth to light extinction. For example a rough rule of thumb is that the Secchi-disk depth corresponds to the depth at which about 85% of the surface light is extinguished (Sverdrup et al. 1942, Beeton 1958). When we assume this level, Eq. 29.23 becomes

$$0.15 = e^{-k_e SD} \qquad (29.24)$$

Further, the extinction coefficient is often related to chlorophyll levels. One common model is a linear proportionality,

$$k_e = k_{we} + \alpha \text{Chl} a \qquad (29.25)$$

where k_{we} = extinction due to water, color, and nonalgal particles (m^{-1}) and α = a coefficient (L μg^{-1} m^{-1}). Substituting this relationship and taking the natural logarithm gives

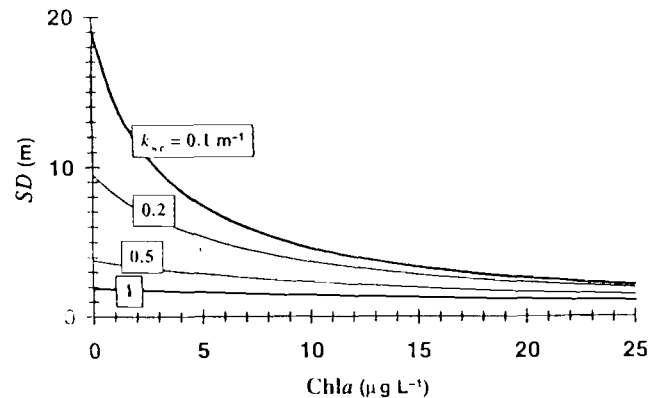$$\ln 0.15 = -(k_{we} + \alpha \text{Chl} a) SD \qquad (29.26)$$

FIGURE 29.7
The relationship between Secchi-disk depth and chlorophyll derived from the Beer-Lambert law and light extinction relationships.

which can be manipulated to give

$$SD = \frac{1}{1 + \mu \text{Chl} a} SD_{max} \qquad (29.27)$$

where $\mu = \alpha / k_{we}$ and $SD_{max} = 1.9 / k_{we}$. Thus the relationship starts at an initial Secchi-disk depth corresponding to particle-free water. Then, as chlorophyll fosters light extinction, the Secchi-disk depth is reduced to zero. Figure 29.7 illustrates this pattern.

29.3.3 Areal Hypolimnetic Oxygen Demand

Rast and Lee (1978) presented the following correlation to predict the areal hypolimnetic oxygen demand in lakes (Fig. 29.8),

$$\log AHOD = 0.467 \log \left[\frac{L}{q_s(1 + \sqrt{\tau_w})} \right] - 1.07 \qquad (29.28)$$

where AHOD = areal hypolimnetic oxygen demand (gO m^{-2} d^{-1}), or taking the antilog,

$$AHOD = 0.0851 \left[\frac{L}{q_s(1 + \sqrt{\tau_w})} \right]^{0.467} \qquad (29.29)$$

Thus even though the equation seems to represent a correlation with loading, it actually correlates AHOD with in-lake total P concentration (recall Eq. 29.13).
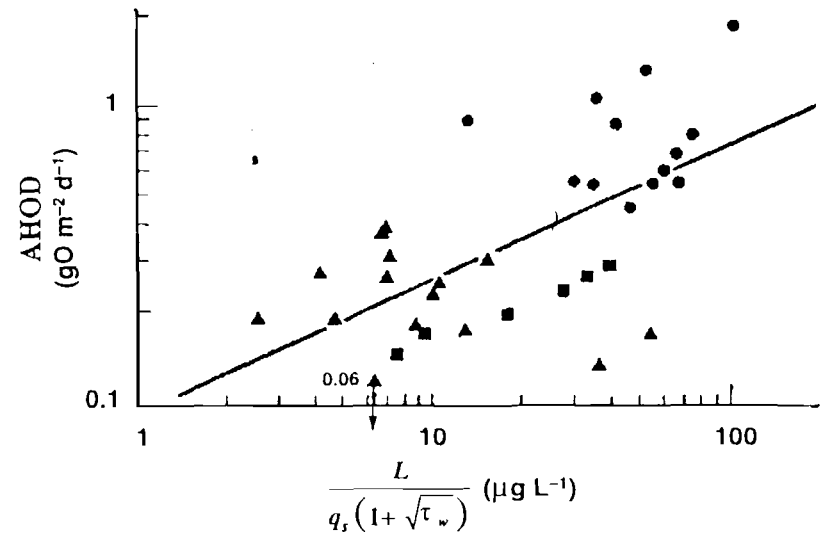

FIGURE 29.8
The relationship between areal hypolimnetic oxygen demand and phosphorus loading (Rast and Lee 1978).

Chapra and Canale (1991) realized this and reanalyzed Rast and Lee's data to determine a direct correlation with total P concentration,

$$AHOD = 0.086 p^{0.478} \qquad (29.30)$$

where p = mean total P concentration of the lake (μgP L^{-1}).

When this equation is plotted on untransformed scales (recall Fig. 25.2b), it traces a saturating curve that suggests that as lakes become more productive, the amount of AHOD does not increase as rapidly as the phosphorus increases. This is consistent with Fair's observation (Fair et al. 1941) that sediment oxygen demand increases as the square of the organic carbon content of a sediment. In addition it conforms to Di Toro et al.'s (1990) SOD model. If it is assumed that lakes with higher total P have higher sediment organic content, Eq. 29.30 and Fair's observation and Di Toro's model show some consistency.

29.3.4 Summary

The models and correlations constituting the phosphorus loading concept have been widely used, in part because they are so easy to apply. They also have the intrinsic appeal of any empirical approach. That is, they directly reflect observations—"what you see, is what you get."

Unfortunately these models and correlations also have shortcomings:

- Because the plots are all log-log and exhibit large scatter, the prediction errors are substantial. In the forms presented here, these errors are not explicitly displayed. Thus the user might naively employ a highly uncertain prediction with unwarranted confidence in its validity. Reckhow (Reckhow 1977, 1979; Reckhow and Chapra 1979, 1983) and Walker (1977, 1980) have addressed this deficiency in detail and offered remedies. Unfortunately because the loading models and plots are so easy to use, uncertainty is rarely connected with the resulting predictions.
- The models are commonly developed from widely heterogeneous data bases. For example lakes from different regions and different types of lakes (e.g., well-mixed lakes and elongated impoundments, some nitrogen-limited systems, etc.) are often included in the same correlation. The net result is that the prediction error becomes inflated by regional and lake-type variability. One remedy is to develop customized correlations for specific lake regions or types.
- They provide little mechanistic insight into the mechanisms underlying the eutrophication process. Further, their utility is limited to the specific applications for which they were intended—that is, simulation and assimilation capacity estimation. In contrast, mechanistic models can be extended to assess environmental modifications (e.g., dredging, reaeration, etc.) and to guide research and experimentation.

In spite of these shortcomings, empirically derived loading models often provide useful order-of-magnitude estimates. As such they provide a quick means to "see the big picture." In other words they offer a way to discern how eutrophication in a particular lake relates to how lakes generally behave.

29.4   SEDIMENT-WATER INTERACTIONS

Bottom sediments have long been acknowledged as a potential source of phosphorus to the overlying waters of lakes and impoundments. As such, sediment feedback could have a significant impact on the recovery of such systems. This would be particularly true in shallow lakes or those with anaerobic hypolimnia.

We have already alluded to sediment feedback of nutrients in Sec. 25.6.4. Such mechanistic frameworks provide one means to simulate the process. In this section we develop an alternative approach that is more akin to the phosphorus loading models described herein. That is, semiempirical formulations are used to simulate sediment feedback in conjunction with simple total phosphorus budgets for the water and the sediments. Such a simplified approach is sometimes more consistent with typical data collection programs for many water bodies.

29.4.1   Sediment-Water Model

In this section we develop a simple modeling framework to address this problem for stratified lakes. The framework, which is expressly designed for management applications, includes two components: a total phosphorus budget and a model of hypolimnetic oxygen deficit. Each is described briefly in the following paragraphs.

Total phosphorus model. A sediment-water model for total phosphorus in a lake and its underlying sediments (Fig. 29.9) can be written as

$$V_1 \frac{dp_1}{dt} = W - Q p_{in} - v_s A_s p_1 + v_r A_s p_2 \qquad (29.31)$$

$$V_2 \frac{dp_2}{dt} = v_s A_s p_1 - v_r A_s p_2 - v_b A_s p_2 \qquad (29.32)$$

where the subscripts 1 and 2 designate the water and the enriched surface sediment layer, respectively, v_s = settling velocity of phosphorus from the water to the sediments (m yr^{-1}), A_s = surface area of the deposition zone (m^2), v_r = recycle mass-transfer coefficient from the sediments to the water (m yr^{-1}), and v_b = a burial mass-transfer coefficient from the enriched surface layer to the deep sediments (m yr^{-1}).
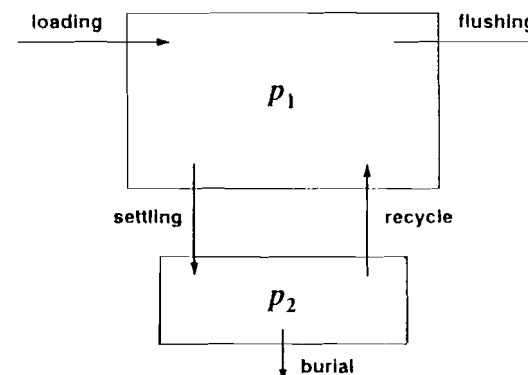

FIGURE 29.9
Schematic diagram of a phosphorus budget model for a lake underlain by sediments.

Hypolimnetic oxygen model. A zero-order model is employed here to simulate hypolimnetic oxygen during periods when the lake is stratified,

$$o_h = o_i - \frac{AHOD}{H_h}(t - t_s) \tag{29.33}$$

where o_h = hypolimnetic dissolved oxygen level (g m^{-3})

o_i = initial oxygen concentration at the onset of stratification (g m^{-3})

AHOD = areal hypolimnetic oxygen demand (g m^{-2} d^{-1})

H_h = average hypolimnion thickness (m)

t = time (d)

t_s = time of onset of stratification (d)

Although frameworks to predict AHOD as a function of the quality of the overlying water are currently under development (Lec. 25), empirical approaches provide a much simpler means to estimate this quantity. For example, Eq. 29.30 can be used.

For dimictic lakes, an AHOD can also be exerted during winter inverse stratification. To simulate depletion for these systems Eq. 29.30 can be extrapolated on the basis of temperature using

$$AHOD_w = AHOD_s 1.08^{T_w - T_s} \tag{29.34}$$

where T_s is the temperature (°C) at which the summer AHOD$_s$ is measured and T_w is the temperature (°C) corresponding to the desired winter AHOD$_w$. Note that a similar temperature correction factor is used to scale the recycle velocity.

29.4.2 Application: Shagawa Lake

Shagawa Lake, Minnesota, is an ideal setting to illustrate the model. This is because it is one of the first systems where sediment feedback was recognized as being important. In addition it has been the subject of numerous studies and, hence, there is a large quantity of information available for model calibration. Finally after being polluted for many years, it was the subject of significant nutrient load reductions in the early 1970s.

Model calibration is based on the extensive data reported by Larsen, Malueg, and colleagues (e.g. Larsen and Malueg, 1976, 1981; Larsen et al. 1975, 1979, 1981; Malueg et al., 1975; Bradbury and Waddington, 1973). Parameter values were determined by calibrating for the pretreatment period for which data is available (1967–1972). As in the following example, it is assumed that the lake was at a steady-state during this time frame.

EXAMPLE 29.1. CALIBRATION OF SEDIMENT-WATER TOTAL P MODEL. Data for Shagawa Lake from 1967 through 1972 are summarized in Tables 29.2 and 29.3. Use this data to calibrate the sediment-water total P model. Specifically, estimate (a) the burial and (b) the recycle velocities.

Solution: If the system is at steady-state, the sources and sinks of phosphorus should balance. As depicted in Fig. E29.1-1, the amount of phosphorus buried must be equal to the difference between phosphorus inflow and outflow.

TABLE 29.2
Data for Shagawa Lake (1967 to 1972)

Parameter	Symbol	Value	Units
Volume	V_1	53×10^6	m^3
Surface area	A_1	9.6×10^6	m^2
Mean depth	H_1	5.5	m
Hypolimnion thickness	H_h	2.2	m
Deposition zone area	A_2	4.8×10^6	m^2
Surface sediment thickness	H_2	10	cm
Total P loading	W_{in}	6692×10^6	mg yr^{-1}
Total P outflow	W_{out}	4763×10^6	mg yr^{-1}
Mean water P concentration	p_1	56.3	mg m^{-3}
Mean sediment P concentration	p_2	500,000	mg m^{-3}
Hypolimnion temperature—summer	$T_{h,s}$	15	°C
Hypolimnion temperature—winter	$T_{h,w}$	4	°C
Total P settling velocity	v_s	42.2	m yr^{-1}
Summer initial hypolimnetic DO	$DO_{i,s}$	8	mg L^{-1}
Winter initial hypolimnetic DO	$DO_{i,w}$	8	mg L^{-1}

TABLE 29.3
Stratification data for Shagawa Lake (1967 to 1972)

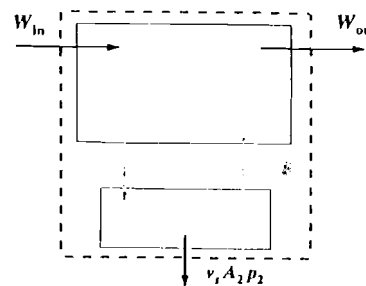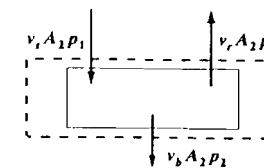| Event	Day
Start of spring mixed period	120
Start of summer stratification	150
Start of fall mixed period	255
Start of winter stratification	320

FIGURE E29.1-1

FIGURE E29.1-2

Thus the burial velocity can be computed as

$$v_b = \frac{W_{in} - W_{out}}{A_2 p_2} = \frac{6692 \times 10^6 - 4763 \times 10^6}{4.8 \times 10^6(500,000)} = 8.03 \times 10^{-4} \text{ m yr}^{-1}$$

(b) The recycle velocity can be estimated by taking a mass balance around the sediments to determine how much phosphorus is recycled from the sediments to the water on an annual basis (Fig. E29.1-2). The balance can be solved for the amount of phosphorus recycled per year,

$$v_r A_2 p_2 = v_s A_2 p_1 - v_b A_2 p_2 = 11,410 \times 10^6 - 1928 \times 10^6 = 9476 \times 10^6 \text{ mg yr}^{-1}$$

Now, this value must be distributed over the summer and winter anoxic periods. To do this we must determine the AHOD rates. For the summer,

$$AHOD = 0.086(56.3)^{0.478} = 0.5905 \text{ g m}^{-2} \text{ d}^{-1}$$

This value along with other parameters can be substituted into Eq. 29.33 to determine how long after stratification the lake would go anoxic (that is, below approximately 1.5 mg L^{-1}),

$$(t - t_s) = \frac{(o_i - o_{anoxic})(H_h)}{AHOD} = \frac{(8 - 1.5)2.2}{0.5905} = 24.2 \text{ d}$$

which means that in the summer the lake will be anoxic for $105 - 24.2 = 80.8$ d. A similar calculation (with the temperature correction from Eq. 29.34) can be used to determine that the lake would be anoxic for 108.5 d during the winter.

The total amount of recycled phosphorus can be set equal to the terms in the model accounting for recycle in the summer and winter anoxic periods,

$$W_{recycle} = F_{a,s} v_r 1.08^{T-T_{h,s}} A_2 p_2 + F_{a,w} v_r 1.08^{T-T_{h,w}} A_2 p_2$$

where $F_{a,s}$ and $F_{a,w}$ = fractions of the year when the hypolimnion is anoxic during summer and winter, respectively. This equation can then be solved for

$$v_r = \frac{W_{recycle}}{A_2 p_2 (\Delta t_{a,s} 1.08^{T_{h,s}-20} + \Delta t_{a,w} 1.08^{T_{h,w}-20})}$$

$$= \frac{9476 \times 10^6}{4.6 \times 10^6(500,000)\left[\frac{80.8}{365}(1.08^{15-20}) + \frac{108.5}{365}(1.08^{4-20})\right]} = 0.01663 \text{ m yr}^{-1}$$

Figure 29.10 shows simulation results for a single year during the steady-state calibration period. Data shown are for 1972 (Larsen et al. 1979). Notice how the phosphorus increases due to the heightened release rate when the oxygen level falls below 1.5 mg L^{-1}. A better fit could have been accomplished by additional tuning of the parameters or by allowing the model parameters to vary seasonally. However, considering the simplicity of the present calibration process, Fig. 29.10 is judged to be an adequate approximation of the general trend of the data.

To obtain some perspective on the long-term dynamics of Shagawa Lake, a simulation was performed for the period from 1880 to 2000. Actual flows were used for the period 1967 to 1979. An average flow is used for all other years.

Because measurements were not made prior to 1967, an idealized long-term loading scenario was developed (Fig. 29.11). Measured loadings are used for the
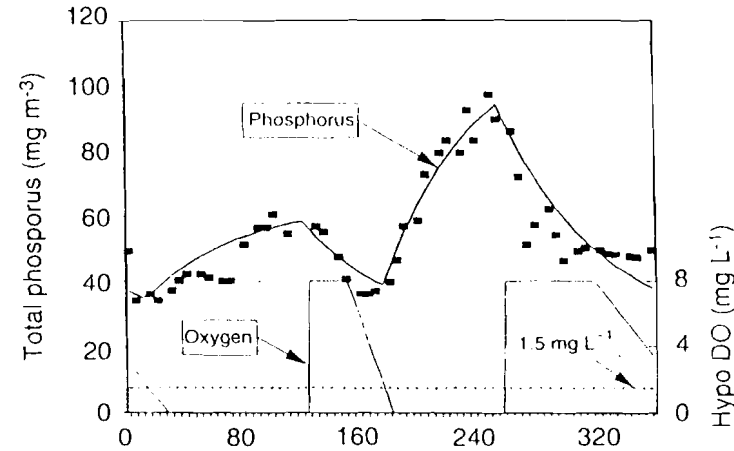
FIGURE 29.10
Plot of phosphorus and oxygen in the pretreatment period (1967–1972) for Shagawa Lake. The data are for 1972 (Larsen et al. 1979).

period 1967 to 1979. Before 1890 and after 1979, an average "natural" loading of 1311 kg yr^{-1} (Larsen et al. 1975) is assumed to apply.

In 1890 the town of Ely was established in the lake watershed. From 1890 to the present, the town's population has been relatively stable. An idealized scenario is used to characterize the town's contribution. The scenario assumes that immediately upon Ely's establishment, the loadings increased stepwise to the high average levels of the late 1960s. Although the actual loading was undoubtedly different from this idealization, in the absence of direct measurements it is considered to be an adequate first approximation.

The results of the long-term simulation along with measured data are shown in Fig. 29.11. The plot indicates that after the 1973 load reduction, the lake experienced an immediate quick response. However, by 1974 the lake's recovery slowed significantly due to feedback of phosphorus from the sediments.

Aside from its simplicity, the use of a step increase to characterize the historical loading scenario allows a clearer visualization of the model's response characteristics. As in Fig. 29.11, the model shows an immediate sharp increase in 1890 following the step load increase. Then, as sediment feedback begins to dominate, the remainder of the increase proceeds at an extremely slow rate (about 0.2 mg m^{-3} yr^{-1}). By the early 1960s, the lake was just beginning to approach a steady-state. Although it had not totally reached a steady-state at that time, it seems to have been close enough to make our calibration acceptable.

The simulation results and data for the recent past are depicted in Fig. 29.12. The adequacy of the simulation can be assessed by three features of the response. First, the model approximately matches the prediversion levels of 50 to 60 mg m^{-3}. Second, the initial rapid drop of about 25 mg m^{-3} is close to the observed drop. Finally, the rate of the subsequent retarded recovery is quite close in the data. Considering that the model parameters are untuned, these results are encouraging.
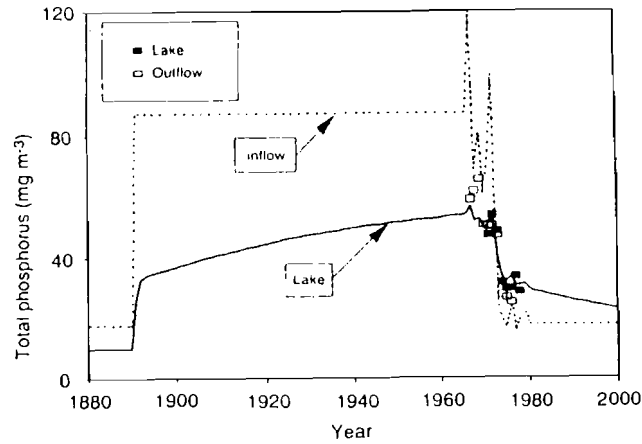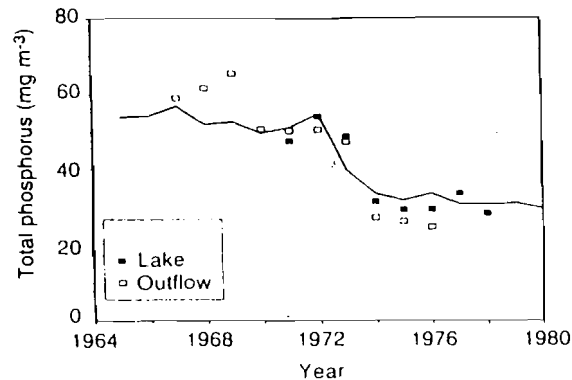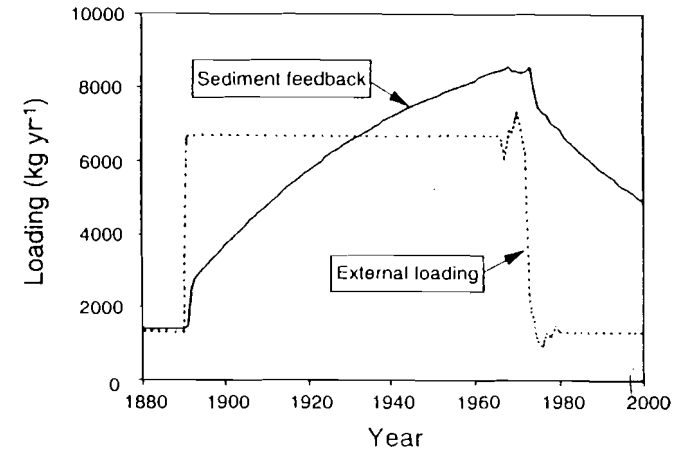
FIGURE 29.11
Long-term total phosphorus concentration for Shagawa Lake as simulated by the phosphorus-oxygen model (thick line). A plot of inflow concentration is superimposed (thin line) for comparison.

FIGURE 29.13
Long-term trends of sediment recycle (thick line) of phosphorus for Shagawa Lake as simulated by the phosphorus-oxygen model. The external loading is superimposed (thin line) for comparison.

Figure 29.13 is a plot of external and internal loadings as calculated by the model. Notice how the internal sediment feedback load takes many decades to build up to the high levels observed during the 1960s. Also notice how after advanced treatment was installed in 1973, the sediment feedback experienced a small abrupt drop followed by a very gradual decrease. It also indicates that, although the constant feedback model would be adequate for short-term projections (that is, less than a decade), long-term predictions would have to account for the gradual decline in sediment release.

In summary the foregoing provides a preliminary framework for assessing the impact of sediment feedback of phosphorus on long-term lake recovery, which because it depends on a few parameter values, offers a simple means to assess the long-term impact of nutrient loadings on lake eutrophication.

29.5 SIMPLEST SEASONAL APPROACH

Temperature changes have a profound effect on mass cycling within the water column. The presence of a strong thermocline essentially divides the lake into two vertical layers with markedly different characteristics (Fig. 29.14).
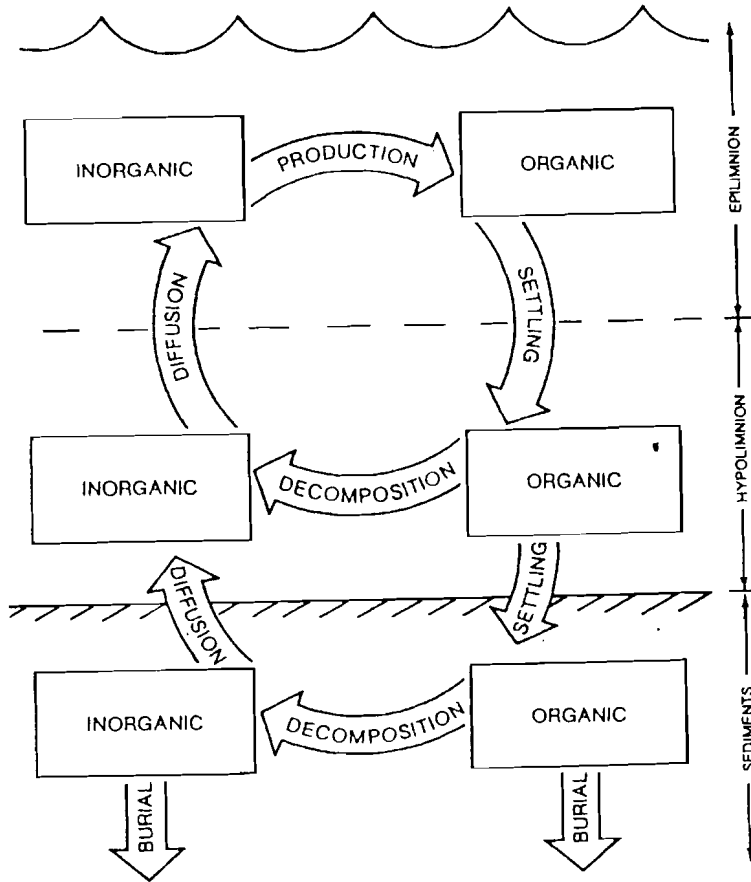
The surface layer (epilimnion) is warm and well-illuminated. Consequently algal photosynthesis leads to transformation of dissolved nutrients into particulate organic matter. Although the thermocline greatly reduces vertical mixing, some of this particulate matter settles and diffuses to the bottom layer (hypolimnion), where it decomposes and eventually returns to a soluble form. Mixing across the thermocline then reintroduces some of the dissolved nutrient to the surface water, where it is again taken up by the phytoplankton. Because many contaminants in lakes are associated with particulate organic matter, this cycle has significance to their transport and fate.

This section describes an approach to simulating basic features of this cycle. The key characteristic of the approach is that it partitions the substance being modeled into two fractions. Although the model is specifically developed for phosphorus, this partitioning is basic to many other substances (such as certain toxic compounds), and the approach could serve as a preliminary framework for analysis of the seasonal dynamics of these contaminants. In addition to its use in simulating mass cycling, the model can also be employed to simulate oxygen concentration in the water column.

29.5.1 Model Formulation

Most of the models described in earlier lectures deal with the dynamics of a single substance in a vertically well-mixed water body. As previously mentioned, many
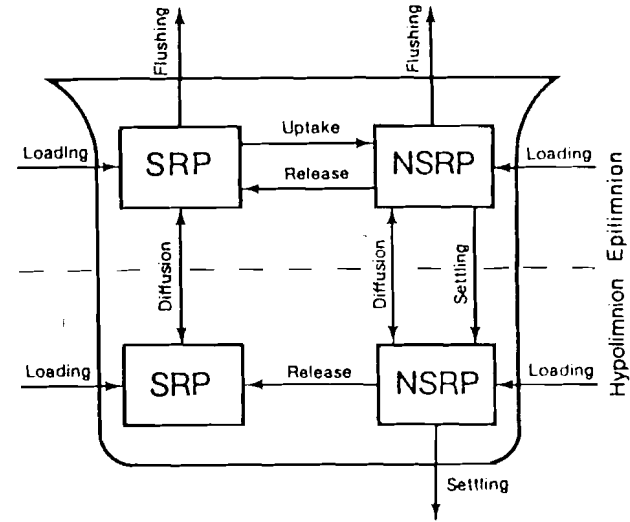

FIGURE 29.12
Recent total phosphorus concentration for Shagawa Lake as simulated by the phosphorus-oxygen model.

FIGURE 29.14
Idealized representation of the cycle of production and decomposition that plays
a critical role in determining the vertical distribution of matter in stratified lakes.

FIGURE 29.15
Schematic representation of the "simplest seasonal approach"
developed by O'Melia, Imboden, and Snodgrass.

constituents occur in various chemical and/or biological forms that are subject to
transformations due to thermal stratification of the water column. O'Melia (1972),
Imboden (1974), and Snodgrass (1974; and O'Melia 1975) have provided a model-
ing framework that makes a first attempt to simulate some of these changes for the
nutrient phosphorus. Simons and Lam (1980) have dubbed this framework the "sim-
plest seasonal approach" or SSA (Fig. 29.15). Although each of their approaches has
unique features (for which the reader can refer to the original publications), in gen-
eral all the models have the following characteristics:

1. Phosphorus is separated into two components. These conventionally refer to
    soluble reactive phosphorus (SRP) and phosphorus that is not soluble reactive

phosphorus (NSRP).[†] This breakdown has an operational basis because the two
most common phosphorus measurements are for SRP and total phosphorus (TP).
NSRP can therefore be estimated by the difference of the two quantities as in
NSRP = TP – SRP. In the model itself a further distinction is made in that NSRP
is subject to settling losses whereas SRP is not. This is based on the assumption
that a significant portion of the NSRP is in particulate form. However, because
NSRP also includes nonsettleable dissolved organic phosphorus (DOP). the dis-
tinction is not precise. We return to the subject of the definition and interpretation
of the phosphorus fractions and the general question of kinetic segmentation at
the end of this section.

2. The lake is segmented spatially into well-mixed upper and lower layers of con-
    stant thicknesses.

3. The year is divided into two seasons representing a summer. stratified period
    during which turbulent exchange between the layers is minimal and a winter,
    circulation period when turbulent transport is intense and the lake is well-mixed
    vertically.

4. Linear first-order differential equations are used to characterize the transport and
    kinetics representing the mass exchange between the components. As schema-
    tized in Fig. 29.15, these exchanges include the following:

[†] Note that Imboden (1974) treats phosphorus as dissolved P available for bioproduction and particulate
P. He therefore does not explicitly account for dissolved organic phosphorus. The question of kinetic
segmentation is explored in further detail at the end of this section.

- *Waste inputs.* Mass loadings of SRP and NSRP fractions can be input to both the epi- and the hypolimnion.
- *Transport.* Flushing of mass through the lake's outlet is characterized mathematically in a similar fashion to a single CSTR (that is, as flow times concentration), yet it differs in that only the surface layer loses mass in this way. A small level of vertical turbulent transfer or diffusion between the layers is used during the stratified period. For the winter, the diffusion coefficient is increased to the point where for all practical purposes the lake is well-mixed.
- *Settling.* By definition, only NSRP is removed from the water column using settling velocity relationships. Separate settling velocities can be input for the two layers as well as for the two seasons.
- *Uptake.* To account for the fact that SRP is transformed into particulate matter via phytoplankton production, uptake of SRP is characterized by a first-order reaction. This mechanism is included only in the epilimnion under the assumption that light limitation makes it negligible in the lower layers. In addition a much higher uptake rate is used during the summer to account for the fact that production is greatest at that time.
- *Release.* A number of mechanisms such as decomposition, respiration, zooplankton grazing, etc., act to return phosphorus from the NSRP to the SRP pool. A first-order reaction dependent on the concentration of NSRP is used to approximate this phenomenon.

To this point the kinetics of most models in this volume have been characterized as simple first-order decay of a single pollutant. With the SSA we begin to introduce more elaborate representations of substance interactions. As in Fig. 29.15, the phosphorus forms are coupled by uptake and release reactions. For example in the epilimnion, phosphorus is lost from the NSRP compartment or "pool" by a release reaction. This loss, in turn, represents a gain for the SRP pool. Therefore, when we write the mass balance for a particular pool, each arrow in Fig. 29.15 represents a term in the resulting differential equation. For example for the SRP pool in the epilimnion,

$$V_e \frac{dp_{s,e}}{dt} = W_{s,e} - Qp_{s,e} + v_t A_t(p_{s,h} - p_{s,e}) - k_{u,e} V_e p_{s,e} + k_{r,e} V_e p_{n,e}$$

$$\text{Accumulation} = \text{Loading} - \text{Flushing} + \quad \text{Diffusion} \quad - \quad \text{Uptake} + \text{Release}$$

$$(29.35)$$

where the subscripts *n* and *s* designate NSRP and SRP fractions, respectively, and the subscripts *e* and *h* designate epilimnion and hypolimnion, respectively.

Although the reactions in Eq. 29.35 are all first-order, they could just as easily be more complicated formulations. For example in Lec. 33, nonlinear relationships are used to characterize phytoplankton growth. In addition if other substances (such as additional forms of phosphorus or other nutrients) were to be included in the model, compartments (each representing a differential equation) and arrows (each representing a term in the differential equation) could be included. The point is that regardless of the complexity of the situation, the conservation of mass, as reflected by the set of differential equations, is a simple bookkeeping exercise to account for how, when, and where mass moves within the system.

TABLE 29.4

Typical ranges of parameters for the simplest seasonal approach for modeling phosphorus

Parameter	Season	Symbol	Range[*]	Units
Epilimnetic uptake rate	Summer	$k_{u,e}$	0.1–5.0	d^{-1}
	Winter	$k_{u,e}$	0.01–0.5	d^{-1}
Epilimnetic release rate	Summer	$k_{r,e}$	0.01–0.1	d^{-1}
	Winter	$k_{r,e}$	0.003–0.07	d^{-1}
Hypolimnetic release rate	Summer	$k_{r,h}$	0.003–0.07	d^{-1}
	Winter	$k_{r,h}$	0.003–0.07	d^{-1}
Settling velocity	Annual	v_e, v_h	0.05–0.6	$m\,d^{-1}$

[*] Values are taken primarily from Imboden (1974) and Snodgrass (1974).

The mass balances for the three remaining pools are

$$V_e \frac{dp_{n,e}}{dt} = W_{n,e} - Qp_{n,e} + v_t A_t(p_{n,h} - p_{n,e})$$
$$+ k_{u,e} V_e p_{s,e} - k_{r,e} V_e p_{n,e} - v_e A_t p_{n,e} \quad (29.36)$$

$$V_h \frac{dp_{s,h}}{dt} = W_{s,h} + v_t A_t(p_{s,e} - p_{s,h}) + k_{r,h} V_h p_{n,h} \quad (29.37)$$

$$V_h \frac{dp_{n,h}}{dt} = W_{n,h} + v_t A_t(p_{n,e} - p_{n,h})$$
$$- k_{r,h} V_h p_{n,h} + v_e A_t p_{n,e} - v_h A_t p_{n,h} \quad (29.38)$$

Definitions and typical values of the parameters are contained in Table 29.4.

29.5.2 Application to Lake Ontario

Parameters for Lake Ontario are summarized in Tables 29.5 and 29.6. In addition the heat exchange coefficient across the thermocline is 0.0744 m d^{-1} during the summer stratified period, and the water column is well-mixed vertically during other times of the year.

Equations 29.35 to 29.38 can be integrated numerically with a method such as the fourth-order Runge-Kutta technique. The results are displayed in Fig. 29.16. As can be seen, the primary feature in the epilimnion is the shift of mass from the SRP and the NSRP fraction during summer due to the large uptake rate. Because of the lack of production, the hypolimnion is generally a more stable system, with concentrations maintained at fairly constant levels throughout the year.

Although the above framework captures many of the essential features of the seasonal cycle, it has several limitations. In particular, its use of constant coefficients and first-order kinetics limits its general applicability. Many of the processes governing substance interactions in the water column are nonlinear and dependent on factors not accounted for in this model. For example the epilimnetic uptake rate depends, among other things, on light intensity, temperature, and levels of both the phytoplankton and the dissolved nutrient. In addition the dependence on the nutrient is described by a nonlinear relationship. Thus some efforts to refine Equations

TABLE 29.5
Information on Lake Ontario in the early 1970s

| Parameter	Symbol	Value	Units
Area			
Surface	A_s	19,000	10^6 m^2
Thermocline	A_t	18,500	10^6 m^2
Mean depth			
Whole lake	H	86	m
Epilimnion	H_e	15	m
Hypolimnion	H_h	71	m
Volume			
Whole lake	V	1634	10^9 m^3
Epilimnion	V_e	254	10^9 m^3
Hypolimnion	V_h	1380	10^9 m^3
Outflow	Q	212	10^9 m^3 yr^{-1}
SRP load			
Epilimnion	$W_{s,e}$	4000	10^9 mg yr^{-1}
Hypolimnion	$W_{s,h}$	0	10^9 mg yr^{-1}
NSRP load			
Epilimnion	$W_{n,e}$	8000	10^9 mg yr^{-1}
Hypolimnion	$W_{n,h}$	0	10^9 mg yr^{-1}

29.35 to 29.38 have focused on more mechanistic characterizations of the kinetic interactions (Imboden and Gachter 1978). Later lectures review nutrient/food-chain models that incorporate sufficient refinements as to constitute an alternative method.

Other ways in which the approach can be modified would be to divide the hypolimnion into several layers to try to resolve vertical gradients in the bottom waters (Imboden and Gachter 1978). In addition the metalimnion can be modeled as a third segment.

Likewise, phosphorus can be subdivided into additional components to more realistically define its dynamics. For example a distinction can be made between living particulate phosphorus and detrital phosphorus or between dissolved organic and dissolved inorganic forms. Figure 29.17 depicts a number of possible kinetic segmentation schemes for phosphorus.

TABLE 29.6
Kinetic parameters for Lake Ontario in the early 1970s

Parameter	Season	Value	Units
$k_{u,e}$	Summer	0.36	d^{-1}
	Winter	0.045	d^{-1}
$k_{r,e}$	Summer	0.068	d^{-1}
	Winter	0.005	d^{-1}
$k_{r,h}$	Summer	0.005	d^{-1}
	Winter	0.005	d^{-1}
v_s, v_h	Annual	0.103	m d^{-1}
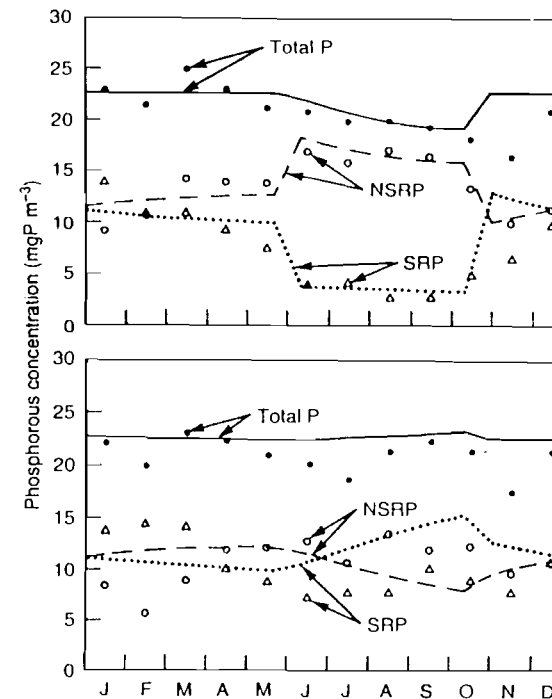
FIGURE 29.16
Data and simulation results using the simplest seasonal approach for total phosphorus in Lake Ontario. (Top—epilimnion; Bottom—hypolimnion).

29.5.3 Kinetic Segmentation

There are three basic rationales underlying kinetic segmentation:

- First, the division of matter can be based on measurement techniques as in the case of the SRP/NSRP scheme. Similarly a dissolved/particulate split (Fig. 29.17b) is, in part, based on the use of filtration to discriminate between these pools.
- Second, the segmentation can have a mechanistic basis. For example the breakdown of matter into pools with similar kinetic characteristics facilitates derivation and measurement of the input-output terms and coupling mechanisms between components. The division of the particulate phosphorus into phytoplankton and detrital components (Fig. 29.17h) is illustrative of this rationale since the settling rates of these two pools are different and can be measured separately.
- Finally the segmentation scheme can have a management basis. For example the explicit formulation of a phytoplankton pool has informational value for the planner trying to assess the deleterious effects of eutrophication.

A general advantage of adding compartments is that the transport and reaction processes can usually be formulated in a more mechanistic manner based on measurements. A disadvantage is that additional effort must be expended to obtain these measurements. In addition the more "sophisticated" representations usually require more effort to program and run on the computer, and they are more difficult to

a)

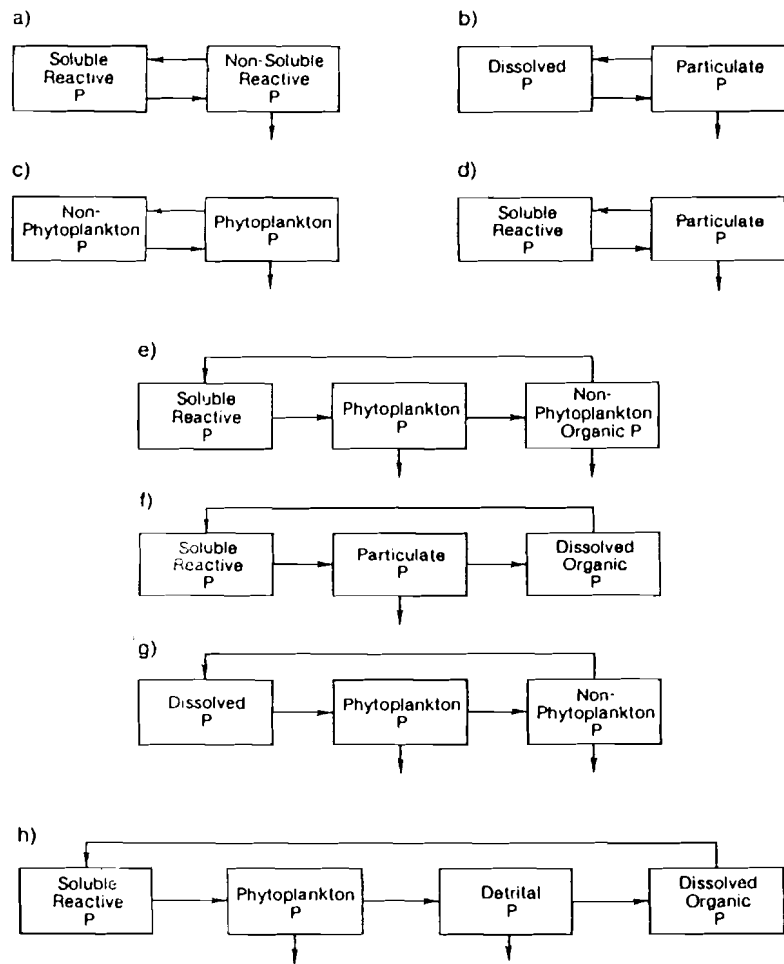
b)

c)

d)

e)

f)

g)

h)

FIGURE 29.17
Alternative kinetic segmentation schemes to model seasonal phosphorus dynamics.

interpret. Further, prediction reliability may actually decrease with additional compartments, because the least understood pools would typically be incorporated last (recall Fig. 18.2). Therefore the decision to expand on a basic framework such as Fig. 29.15 must be made only after considering these factors.

PROBLEMS

29.1. A gravel company excavates a 405-ha gravel pit that is 1.52 m deep. The pit is filled with groundwater at a rate of 100 m³ d⁻¹. The groundwater is devoid of nutrients. The pit has a small drainage area of 607 ha. Rainfall on this drainage area yields runoff of

25 cm yr⁻¹ with a phosphorus content of 40 kg km⁻² yr⁻¹. Atmospheric sources of total phosphorus are 24 kg km⁻² yr⁻¹. If total phosphorus settles at a rate of 12 m yr⁻¹, calculate the pit's total phosphorus concentration. Note that evaporation exactly equals direct precipitation.

29.2. A lake (surface area = 10⁶ m³, mean depth = 5 m, residence time = 2 yr) has a total phosphorus loading of 2.5 × 10⁸ mg yr⁻¹. Note that the lake has a k_{wc} = 0.15 m⁻¹. Determine the following:

(a) Total phosphorus inflow and lake concentrations
(b) Chlorophyll a concentration
(c) Secchi-disk depth
(d) Loading required to maintain the lake at the border between oligotrophy and mesotrophy

29.3. A stratified lake (surface area = 1.5 × 10⁶ m², thermocline area = 1 × 10⁶ m², epilimnion volume = 1×10⁷ m³, hypolimnion volume = 0.8×10⁷ m³, residence time = 3 yr) has a total phosphorus loading of 7 × 10⁸ mg yr⁻¹. Determine its total P and chlorophyll a concentrations and its Secchi-disk depth. Also, calculate its AHOD and determine the concentration of oxygen in its hypolimnion over the summer stratified period of 3 months.

29.4. Lake Sammamish, located in Washington State, has the following characteristics:

Lake surface area = 119.8 km²	Flow = 2.03 × 10⁸ m³ yr⁻¹
Sediment surface area = 13.068 km²	Active sediment thickness = 10 cm
Water volume = 3.5 × 10⁸ m³	Sediment porosity = 0.9
Hypolimnion volume = 9.8 × 10⁷ m³	Sediment density = 2.5 × 10⁶ g m⁻³
Hypolimnion thickness = 7.5 m	

The lake was heavily polluted in the 1960s when the total P concentration in the lake was approximately 33 mg m⁻³. At this time the lake's inflow concentration was about 100 mg m⁻³. The sediment P concentration at the same time was about 0.12% P.

The lake is monomictic with a stratified period from day 135 to day 315. The oxygen at the beginning of the stratified period is about 8 mg L⁻¹ and the summer hypolimnetic temperature is approximately 10°C.

In 1969 the inflow concentration was abruptly dropped to 65 mg m⁻³. The following data are available for lake total P (in mg m⁻³) before and after the diversion:

Year	1964	1965	1966	1971	1972	1973	1974
Total P	32	35	32	27	29	32.5	25.5
Year	1975	1979	1981	1982	1983	1984	
Total P	20	14	22.5	18.5	16.5	18.5	

If a value of 46 m yr⁻¹ is assumed for the settling velocity, calibrate and simulate total P in this lake from 1960 through the year 2000. Present your results graphically. In addition investigate the response if the inflow concentration had been dropped to 45 or 25 mg m⁻³ in 1969.

29.5. Use the simplest seasonal approach to determine the concentrations in Lake Ontario over the annual cycle if the loadings in the early 1970s were doubled.